Final Draft
of the original manuscript:

Srinivasan, B.; Liang, J.; Balajee, R.; Blawert, C.; Stoermer, M.; Dietzel, W.:

Effect of pulse frequency on the microstructure, phase composition and corrosion performance of a phosphate-based plasma electrolytic oxidation coated AM50 magnesium alloy

In: Applied Surface Science (2010) Elsevier

DOI: 10.1016/j.apsusc.2010.01.052

Effect of pulse frequency on the microstructure, phase composition and corrosion performance of a phosphate-based plasma electrolytic oxidation coated AM50 magnesium alloy

P. Bala Srinivasan*, J. Liang, R.G. Balajeee, C. Blawert, M. Störmer, W. Dietzel
Institute of Materials Research
GKSS-Forschungszentrum Geesthacht GmbH
D-21502, Geesthacht
Germany

*Corresponding Author (bala.srinivasan@gkss.de);
Phone: 00-49-4152-871997; Fax: 00-49-4152-871960

Keywords
Magnesium alloy; plasma electrolytic oxidation; pulse frequency; microstructure; phase composition; corrosion behaviour.

Abstract
An AM50 magnesium alloy was plasma electrolytic oxidation treated using a pulsed DC power supply at three different pulse frequencies viz., 10 Hz, 100 Hz and 1000 Hz with a constant pulse ratio for 15 minutes in an alkaline phosphate electrolyte. The resultant coatings were characterized by X-ray diffraction, energy dispersive spectroscopy and scanning electron microscopy for their phase composition and microstructural features. The 10 Hz condition yielded relatively thick and rough coatings, which was attributed to the higher energy input per individual pulse during the PEO processing. The phase composition was also found to be influenced by the processing frequency. Electrochemical impedance spectroscopy studies performed in 0.1 M NaCl solutions revealed that the coatings produced at 10 Hz condition had a better corrosion resistance, which was attributed to the higher thickness, more compact microstructural features and a relatively stable phase composition.

Introduction
Surface treatments for components made of magnesium alloys are aimed at improving their corrosion resistance and tribological behaviour in order to enhance their life expectancy and service performance in engineering applications [1]. A variety of surface modification procedures have been attempted for the protection of magnesium alloys [2-6]. Amidst these, plasma electrolytic oxidation (PEO) is one of the most preferred techniques as it is capable of producing dense, thick, non-conducting, hard, wear/corrosion resistant ceramic layers on the surface of magnesium alloys [7]. In PEO processing, the electrolytes employed must be capable of forming a passive film, which subsequently should facilitate sparking in order to promote the growth of a ceramic oxide layer on the surface. Alkaline electrolytes containing silicates and/or phosphates are quite popular for the PEO processing, and a large number of studies have been made to understand the structure-property relationships of the PEO coatings produced using these electrolytes on a variety of magnesium alloys [8-11]. In addition to phosphate, silicate and aluminate coatings, recently attempts have been made to produce zirconate coatings on magnesium alloys from acidic electrolytes [12-13]. The

role of additives on the formation and performance of coatings were reported by many researchers. Liang et al. [14-15], investigated the effect of fluoride and tungstate on the characteristics of resultant coatings on AM60B magnesium alloy. Bai and Chen [16] reported the beneficial influence of hexamethylenetetramine and borate as additives in controlling the cracks and improving the corrosion resistance of PEO coatings. The growth of PEO coatings in aluminate-fluoride electrolyte was investigated by Guo and An [17]. In addition to the efforts in fine tuning the PEO processing by appropriate selection of electrolytes, there have been conscious attempts to identify appropriate power sources and processing conditions to produce high-performance coatings. PEO coatings on magnesium alloys are made using AC, DC and bi-polar power sources [18-20]. The role of ultrasonic power to supplement the PEO processing has also been investigated [21]. There is not much published information on the effect of pulse frequency on the characteristics of PEO coatings on magnesium alloys except for a publication of Lv et al. [22]. The current work is an attempt to understand the effect of processing (pulse) frequency with a constant pulse-time (on-off) ratio, on the formation of PEO coatings on an AM50 magnesium alloy and to characterize the resultant coatings for their microstructure, phase composition and corrosion behaviour.

Experimental

Specimens of size 15 x 15 x 4 mm^3 from an AM50 alloy with a nominal composition of (mass fraction) 4.4% ~ 5.5% Al, 0.26% ~ 0.6% Mn, max 0.22% Zn, max 0.1% Si, and Mg balance were employed in this investigation. They were ground successively with 500, 800, 1200 and 2500 grit emery sheets and cleaned with acetone before the PEO treatment. The plasma electrolytic oxidation process was carried out using a pulsed DC electrical power source in a phosphate based electrolyte containing 1 g of potassium hydroxide and 10 g sodium phosphate in one liter of distilled water. The coatings were obtained at a constant current density of 30 $mA{\cdot}cm^{-2}$ for 30 minutes at three frequencies viz., 10, 100 and 1000 Hz, with a fixed on-off pulse-time ratio of t_{on}/t_{off} = 1:9 (i.e. 10 ms:90 ms, 1 ms:9 ms and 0.1 ms:0.9 ms, respectively). The temperature of the electrolytes during the processing was always kept at 10 $\pm$ 2°C by a water cooling system.

The thickness and roughness of the coatings were assessed using a MiniTest 2100 eddy current meter and a Hommel profilometer, respectively. The surface morphology of the PEO coated specimens was examined in a Cambridge stereoscan scanning electron microscope (SEM). X-ray diffraction (XRD) was performed using a Bruker X-ray diffractometer with Cu-Kα radiation to determine the phase composition. The elemental composition of the PEO coated specimens was assessed in a Zeiss Ultra 55 scanning electron microscope equipped with an energy dispersive X-ray spectrometer (EDS).

Electrochemical impedance spectroscopy (EIS) studies were carried out using a Gill AC potentiostat/frequency response analyser with a typical three electrode cell set-up. The measurements were made at the open circuit potential with an AC amplitude of 10 mV over a frequency range of 0.01 Hz to 30 kHz on the PEO coated specimens exposed to 0.1 M NaCl solution for different durations viz., 0.5, 2, 5, 10, 25 h and 50 h. The corroded surfaces were examined in a stereo-microscope and SEM to understand the extent of corrosion damage.

Results and Discussion

Figure 1 shows the voltage evolution plot as a function of PEO processing time at three different operating frequencies. During PEO processing four different stages viz.,

(i) initial dissolution/passive film formation, (ii) breakdown of passive film and evolution of fine discharges, (iii) transitory phase involving changes in shape, size, density and colour of moving sparks and (iv) the stage of long-lived large-sized sparks of reduced density, were observed in the various ranges as is presented in **Table 1**.

Table 1 Stages of PEO process at three different pulse frequencies

Frequency	Stage 1	Stage 2	Stage 3	Stage 4
10 Hz	Up to ~245 V	245 V – 300V	300 V – 450 V	450 V – 490 V
100 Hz	Up to ~245 V	245 V – 385 V	385 V – 475 V	475 V – 500 V
1000 Hz	Up to ~245 V	245 V – 400 V	400 V – 500 V	500 V – 515 V

The processing frequency did not seem to influence the breakdown voltage, and the breakdown/sparking was observed at around 245 V in all the three conditions. In the 10 Hz condition, between 2 minutes and 5 minutes of treatment time, the voltage was found to increase from 280 V to around 360 V, with a high degree of fluctuation/ instability in voltage. There were slight oscillations in the current value, too, despite the fact that the process was performed at a constant current density. With passage of time, the voltage ramped up slowly to reach a value of 450 V in 15 minutes. From then on, until the end of treatment time, i.e. 30 minutes, the voltage increase was slowed down further to reach a final value of 490 V.

In the case of 100 Hz condition, the voltage increased quickly from the point of breakdown to around 380 V, and thereafter slowed down a bit to reach a value of around 475 V in 10 minutes. Between 10 minutes and 30 minutes, the rise in voltage was only around 25 V, registering a final value of 500 V. On the other hand, in the 1000 Hz case, in the first two stages the voltage shot up to 400 V. The third stage was observed between 400 V and 500 V, and a final working voltage of 515 V was registered in this case.

The sparking characteristics at all the three frequencies were different. The plasma discharges on the surface of the specimen in the 10 Hz condition appeared like a sheath – which was essentially on account of an overlap of numerous very large sized discharges. On the other hand, in the 1000 Hz condition the sparks were much finer and the discharge density was higher at all four stages of processing. In the 100 Hz condition, the sparking characteristics resembled those of the 1000 Hz condition, with the occurrence of discrete individual discharges of moderate size and density. The formation of sheath-like discharges appeared to be only characteristic of the 10 Hz condition.

The effect of processing at the three frequency levels on the surface morphology of the resultant coatings can be observed in the scanning electron micrographs presented in **Figures 2(a) – (c)**. The surface of the specimen PEO coated at the 10 Hz condition contained more or less a similar level of pore density (Figure 2a) as that of the coating obtained in the 100 Hz condition (Figure 2b). However, the size of the pores was larger in the coating obtained at 10 Hz. Both these specimens were found to have large sized micro-cracks on the surface. On the other hand, the specimen coated at 1000 Hz had a much higher pore density, constituted with smaller and uniformly distributed pores. The majority of the pores were found to have been filled with coating compounds, as can be seen in Figure 2c. This surface, too, had numerous micro-cracks. Nevertheless, the crack sizes were very small compared to those observed in the specimens coated at 100 Hz and 10 Hz conditions. The differences in the extent of micro-cracking in the three coatings can be attributed to the differences in the intensity of energy at these processing conditions. Even though the pulse ratio was the same in all the three cases,

the discrete pulse-on-time was only 0.1 ms in the 1000 Hz case, which was lower by one and two orders of magnitude when compared to the 100 Hz and 10 Hz conditions, respectively. This means that the energy per pulse was less in the 1000 Hz condition, and that has resulted in a coating with relatively smaller sized micro-cracks.

The thickness and surface roughness (R_a) of the PEO coatings produced under different conditions are presented in **Figure 3**. The average mean-surface roughness of the 10 Hz coating was 5.7 μm as against values of 3.5 μm and 2.4 μm for the coatings obtained at 100 Hz and 1000 Hz, respectively. The higher surface roughness is attributed to the higher energy density per pulse, which has apparently caused a more intense melting and the consequent formation of the ceramic oxide coating on the surface of the specimen processed at lower frequencies. The lower energy per individual pulse at 1000 Hz condition was not only beneficial in minimizing the micro-cracks, but has also significantly influenced the surface roughness of the coatings.

The thickness was found to be high in the coating produced at 10 Hz, as could be observed from figure 3. It is evident that that the high energy per pulse was responsible for the higher degree of plasma-chemical reactions, leading to a higher thickness of the coatings. Liang et al. **[23]** studied the effect of current density waveform on the formation of PEO coating on a magnesium alloy in a silicate based electrolyte. They reported that the higher energy density led to an increased sparking discharge intensity caused by the pulse energy. They produced coatings with a thickness of 37 μm under three conditions viz., constant, decaying and stepped current conditions. In the decaying and stepped current conditions the time required to achieve the desired thickness was much higher, meaning that the constant current density provided a higher energy for the rapid growth of the coating. Further, in the higher growth rate conditions they observed a higher roughness on the PEO coated surface. In the current work, the increased pulse-on-time in the low frequency conditions was responsible for the higher energy per pulse and hence this had facilitated a higher growth rate. Lv et al., **[22]** have reported a significant drop in the coating growth rate when the operating frequency was increased from 100 Hz to 800 Hz in the PEO processing of a magnesium alloy in a phosphate based electrolyte. The coating produced by them at the higher frequency was reported to have a fine pore size with a higher pore density, which is consistent with the observations of the current work.

The scanning electron micrographs showing the cross-sections of the coatings obtained at difference frequency conditions are shown in **Figures 4 (a) – (c)**. All the three coatings contained a number of discharge pores filled with coating compounds and a few globular pores which might be a result of gas inclusion. The size of the discharge pores observed in the cross-section was tiny in the coating obtained at 1000 Hz condition (Figure 4c). The variations in thickness within the respective coatings are also evident in these micrographs, and these observations corroborate the eddy current probe thickness measurements.

The X-ray diffraction patterns of the coatings obtained at the three frequency conditions are depicted in **Figure 5**. It is apparent that the 10 Hz coating was constituted with MgO and $Mg_3(PO_4)_2$ phases. The XRD pattern of the coating obtained at 100 Hz showed that it was composed predominantly with MgO phase. However, a little mound observed in the 2θ range of 20° – 35° indicated the presence of an amorphous phase, possibly containing phosphorus. A couple of tiny peaks of $Mg_3(PO_4)_2$ identified in this region substantiate the above claim. However, in the 1000 Hz coating, only the MgO was observed. The appearance of magnesium peaks in all three conditions is due to

the employment of incident X-ray technique in which the X-ray has penetrated the coating and reached the substrate.

In order to determine the phosphorous content in the coating, EDS analysis was performed on the surface of all the coated specimens and the results are presented in **Figures 6(a) – (c)**. It was found that the phosphorous content was decreasing with increasing processing pulse frequency. The resultant coatings had a phosphorous content of 18.31, 14.87 and 10.85 at.% in the 10 Hz, 100 Hz and 1000 Hz conditions, respectively. The concentration of sodium was also found in the decreasing order in the coatings as a function of increasing frequency. This confirms the effective participation of Na^+ and PO_4^{3-} ions in the PEO process at lower frequency conditions, which again is attributed to the relatively longer pulse-on-time, providing a higher energy per pulse in the 10 Hz condition. The identification of appreciable amounts of phosphorous, i.e. about 15% and 11% in the coatings produced at 100 Hz and 1000 Hz conditions corroborates the occurrence of an amorphous peak in the 20°– 35° (2θ) range in the XRD spectra for the respective specimens.

The electrochemical corrosion behaviour of the PEO coated specimens was assessed by EIS in a 0.1 M NaCl solution. The EIS results were fitted with two different equivalent circuit (EC) models. For the specimen PEO coated at 10 Hz, the EIS data obtained at all the test durations viz., 0.5, 2, 5, 10, 25 and 50 h could be fitted with a two time constant model as shown in **Figure 7a**. For the specimens PEO coated at 100 Hz and 1000 Hz, the initial EIS (up to 10 h) could be fitted with the EC shown in Figure 7a. However, for the EIS data obtained at the 50 h and 25 h test durations for the 100 Hz and 1000 Hz specimens, respectively, an equivalent circuit model having only one time constant with an additional inductive circuit element as shown in **Figure 7b** was employed. In the equivalent circuits, R_s is the solution resistance, R_p is the resistance of the porous regions of the PEO coating paralleled with constant phase element $(CPE)_p$, R_i is the resistance of the PEO coating, including the resistance of the coating/substrate interface in parallel with $(CPE)_i$, R_f is the resistance of the film formed on the magnesium substrate exposed to the corrosive electrolyte in parallel with $(CPE)_f$, and R_L is the charge transfer resistance of pitting corrosion in series with the inductance L.

The Bode plots of the PEO coated specimens (10 Hz) after different durations of exposure to the corrosive environment are shown in **Figure 8(a)** and the corresponding electrochemical parameters are presented in **Table 1**. The resistance of the PEO coating (R_i) in the EIS test after 0.5 h of immersion was 2.5 E5 $\Omega \cdot cm^2$, with the resistance of the porous region (R_p) was 4.5E4 $\Omega \cdot cm^2$. The resistance of the porous region was found to increase slightly in the tests after 2h and 5h immersion, and started to come down drastically after that. The increase in resistance in the 2h/5h tests is attributed to the formation of corrosion products and the filling of the pores. However, with prolonged exposure, the degradation proceeded further in the pores, and the pore resistance started to decrease. Similarly, the resistance of the compact regions of the PEO coating was found to be increase marginally after 2 h. With prolonged exposure this resistance also found to drop marginally to lower values. However, the resistance of the coating (R_i) was reasonably high in the EIS test even after the 50 h of immersion and this coating had resisted the test duration without any significant degradation/ damage.

The Bode plots of the PEO coated specimens at 100 Hz and the corresponding electrochemical data are presented in **Figure 8(b)** and **Table 2**, respectively. Even though the R_p and R_i values in the test after 0.5 h of exposure was slightly higher than that of the specimen coated at 10 Hz, the respective resistance values decreased

rapidly to 220 Ω·cm² and 5.4 x 10^4 Ω·cm² after 10 h of exposure. The values dropped to still lower values in the tests after 25 h of exposure. In the test after 50 h of exposure an inductive loop was observed for this specimen (in the Nyquist plot), which suggested a localized damage on the surface of the coated specimen and the consequent adsorption of chloride ions in the damaged regions.

Like the other two, the specimen coated at 1000 Hz also exhibited a good corrosion resistance in the initial EIS test after 0.5 h of immersion, but the resistance values dropped significantly in the tests after 10 h **(Figure 8(c))**. This coating was found to fail with a localized damage after 25 h of exposure, as evidenced by inductive loops in the EIS spectra. The results of the EIS tests revealed that the 1000 Hz coating was inferior in terms of corrosion resistance despite the fact that this coating had a relatively smooth surface, fine pores and small sized micro-cracks. The coating produced at 10 Hz condition contained MgO and appreciable amounts of $Mg_3(PO_4)_2$ phase compared to the coating produced at 100 Hz condition. The coating produced at 1000 Hz was constituted predominantly with MgO only. Thus, it appears that the corrosion resistance of the PEO coated specimens was governed mainly by the thickness and phase composition and that the 10 Hz coating with a higher thickness/good amounts of $Mg_3(PO_4)_2$ phase offered a superior resistance to the magnesium substrate.

Optical macrographs and scanning electron micrographs showing the surface appearance of the EIS tested specimens are presented in **Figures 9(a)-(f)**. The specimen PEO coated at 10 Hz did not show any sign of localised damage, and macroscopically the surface was found to be intact (Figure 9(a)). Examination of this surface at a higher magnification in SEM revealed that there was no evident degradation of the coating (Figure 9(b)). The specimen coated at 100 Hz was found to have localised damage (Figure 9(c)), which was also reflected by the inductive loop in the impedance plot. The higher magnification micrograph in Figure 9(d) clearly shows the extent of damage on this coated surface. The regions adjoining the damaged zone in the exposed area was found to be free from any perceptible corrosion damage as was in the case of 10 Hz specimen. Even though the 1000 Hz specimen was EIS tested only for 25 h, the surface had a relatively large sized localised damage (Figure 9(e)), and the extent of damage corroborates the EIS data as well. In this specimen, in addition to the formation of a large localised damaged region (Figure 9(f)), a few regions of minor localised damage could also be observed. As like the other two specimens, in this case too, a major portion of the surface area of the coating exposed to the corrosive environment remained unaffected.

The EIS data and the analysis of the corroded surface shows that the coating produced at low frequency (10 Hz) condition was more stable than the rest, and that this coating survived 50 h of exposure to the corrosive environment (0.1 M NaCl). Lv et al., **[22]** reported that a 4 μm thick phosphate based coating produced at 800 Hz had a superior corrosion resistance than a 26 μm thick coating obtained at 100 Hz. They attributed that to the more compact nature of the coating produced at 800 Hz. The coating growth rate was much slower in their attempt, and the processing was much longer than that in the current investigation. The coatings produced at a higher frequency (1000 Hz) in this work exhibited a poor corrosion resistance, contrary to the observations of Lv et al. **[22]**.

It has been reported that the silicate based PEO coating with a higher thickness produced at a higher current density level was found to have an inferior corrosion resistance owing to the higher degree of defects, than that produced at a low current density **[24]**. In another work, a thicker PEO coating obtained from a phosphate based electrolyte was reported to exhibit an inferior corrosion behaviour to that of a relatively

thin silicate based PEO coating [25]. Yet another investigation showed that the phase composition of the PEO coatings influenced the long-term corrosion behaviour significantly [26]. Thus, from our earlier investigations and the current work it is understood that the long term corrosion resistance of the PEO coatings is dictated by the phase composition, thickness, compactness and the level of defects, either individually or synergistically. In this work, the higher energy per pulse in the 10 Hz condition not only had favoured a rapid growth facilitated by a better plasma chemical reactions/sintering, but also influenced the phase composition by promoting the incorporation of $Mg_3(PO_4)_2$ phase in the coating. Hence, it is appropriate that the superior corrosion resistance of the 10 Hz coating is attributed to the (a) phase composition, (b) compact structure with relatively less pore density and (c) higher thickness of the coating.

Conclusions

1. PEO processing at higher frequency (1000 Hz) results in a smooth surface with fine microstructure/surface morphological features.

2. The growth rate of coatings is higher at lower frequency (10 Hz).

3. Higher energy per pulse due to longer on duration in the low frequency condition facilitates not only a higher growth rate but a better sintering of the coating as well. In addition, the intense plasma-chemical reactions at this condition also promote the formation of additional phases which are not formed at higher frequency conditions.

4. Amidst the three coatings investigated, a more compact and higher thickness coating containing MgO and $Mg_3(PO_4)_2$ phases obtained at 10 Hz condition offered the superior corrosion resistance.

Acknowledgement

P. Bala Srinivasan and J. Liang express their sincere thanks to the Hermann-von-Helmholtz Association, Germany, and DAAD, Germany, for the award of fellowship and funding. The technical support of Mr. V. Heitmann, Mr. U. Burmester and Mr. V. Kree during the course of this work is gratefully acknowledged.

References

1. J.E. Gray, B. Luan, Journal of Alloys and Compounds, 336 (2002) 88.

2. K. Brunelli, M. Dabala, I. Calliari, M. Magrini, Corrosion Science, 47 (2005) 989.

3. A. Bakkar, V. Neubert, Electrochemistry Communications, 9 (2007) 2429.

4. Z. Liu, W. Gao, Surface and Coatings Technology, 200 (2006) 3553.

5. S. Sathiyanarayanan, S. Azim, G. Venkatachari, Applied Surface Science, 253 (2006) 2113.

6. C. Blawert, D. Manova, M. Störmer, J.W. Gerlach, W. Dietzel, S. Mändl, Surface and Coatings Technology, 202 (2008) 2236.

7. C. Blawert, W. Dietzel, E. Ghali, G. Song, Advanced Engineering Materials, 8 (2006) 511.

8. P. Su, X. Wu, Y. Guo, Z. Jiang, Journal of Alloys and Compounds, 475 (2009) 773.

9. H. Guo, M. An, S. Xu, H. Huo, Materials Letters, 60 (2006) 1538.

10. R. Arrabal, E. Matykina, F. Viejo, P. Skeldon, G.E. Thompson, Corrosion Science, 50 (2008) 174.

11. J. Liang, B. Guo, J. Tian, H. Liu, J. Zhou, W. Liu, T. Xu, Surface and Coatings Technology, 199 (2005) 121.

12. Z. Yao, H. Gao, Z. Jiang, F. Wang, Journal of American Ceramic Society, 91 (2008) 555.

13. W. Mu, Y. Han, Surface & Coatings Technology, 202 (2008) 4278.

14. J. Liang, B. Guo, J. Tian, H. Liu, J. Zhou, T. Xu, Applied Surface Science, 252 (2005) 345.

15. J. Ding, J. Liang, L. Hu, J. Hao, Q. Xue, Transactions of Nonferrous Metals Society of China, 17(2007) 244.

16. A. Bai, Z. Chen, Surface and Coatings Technology, 203 (2009)1956.

17. H.F. Guo, M.Z. An, Applied Surface Science, 246 (2005) 229.

18. E. Matykina, R. Arrabal, P. Skeldon, G. E. Thompson, Journal of Applied Electrochemistry, 38 (2008) 1375.

19. J. Qian, C. Want, D. Li, B. Guo, G. Song, Transactions of Nonferrous Metals Society of China, 18 (2008) 19.

20. F. Jin, P. Chu, G. Xu, J. Zhao, D. Tang, H. Tong, Materials Science and Engineering, A 435–436 (2006) 123.

21. X.W. Guo, W.J. Ding, C. Lu, C.Q. Zhai, Surface and Coatings Technology, 183 (2004) 359.

22. H. Lv, H. Chen, W.C. Gu, L.Li, E.W. Niu, Y.H. Zhang, S.Z. Yang, Journal of Materials Processing Technology, 208 (2008) 9.

23. J. Liang, L. Hu, J. Hao, Applied Surface Science, 253 (2007) 6939.

24. P. Bala Srinivasan, J. Liang, C. Blawert, M. Störmer, W. Dietzel, Applied Surface Science, 255 (2009) 4212.

25. J. Liang, P. Bala Srinivasan, C. Blawert, M. Störmer, W. Dietzel, Electrochimica Acta, 54 (2009) 3842.

26. J. Liang, P. Bala Srinivasan, C. Blawert, W. Dietzel, Corrosion Science, 51 (2009) 2483.

Table 1 EIS fit results for the specimens PEO coated at 10 Hz

Immersion time	$(CPE\text{-}T)_p$	$(CPE\text{-}P)_p$	R_p ($\Omega\cdot cm^2$)	$(CPE\text{-}T)_i$	$(CPE\text{-}P)_i$	R_i ($\Omega\cdot cm^2$)
0.5h	1.2E-6	0.64	4.5E4	7.6E-6	0.52	2.5E5
2h	2.6E-6	0.60	6.4E4	9.6E-6	0.67	2.6E5
5h	5.3E-6	0.66	7.5E4	1.6E-5	0.69	1.8E5
10h	8.8E-6	0.62	630	9.6E-7	0.93	1.5E5
25h	1.2E-6	0.88	130	9.9E-6	0.76	1.4E5
50h	3.1E-6	0.83	95	8.8E-6	0.79	1.1E5

Table 2 EIS fit results for the specimens PEO coated at 100 Hz

Immersion time	$(CPE\text{-}T)_p$	$(CPE\text{-}P)_p$	R_p ($\Omega\cdot cm^2$)	$(CPE\text{-}T)_i$	$(CPE\text{-}P)_i$	R_i ($\Omega\cdot cm^2$)
0.5h	6.9E-7	0.69	1.8E5	4.4E-6	0.43	4.4E5
2h	1.6E-6	0.66	2.3E3	1.2E-7	0.94	1.2E5
5h	3.3E-6	0.72	380	1.5E-6	0.89	5.4E4
10h	4.0E-6	0.76	220	3.5E-6	0.88	5.4E4
25h	3.0E-6	0.86	110	7.0E-6	0.86	2.7E4

Immersion time	$(CPE\text{-}T)_f$	$(CPE\text{-}P)_f$	R_f ($\Omega\cdot cm^2$)	L (H)	R_L ($\Omega\cdot cm^2$)
50h	1.7E-5	0.76	7.3E3	4.5E3	1.4E4

Table 3 EIS fit results for the specimens PEO coated at 1000 Hz

Immersion time	$(CPE\text{-}T)_p$	$(CPE\text{-}P)_p$	R_p ($\Omega\cdot cm^2$)	$(CPE\text{-}T)_i$	$(CPE\text{-}P)_i$	R_i ($\Omega\cdot cm^2$)
0.5h	4.4E-6	0.60	2.3E4	3.3E-6	0.72	1.6E5
2h	9.8E-6	0.61	940	2.3E-7	0.93	1.5E5
5h	9.8E-6	0.71	270	9.0E-7	0.98	7.4E4
10h	8.3E-6	0.75	90	2.2E-6	0.94	5.1E4

Immersion time	$(CPE\text{-}T)_f$	$(CPE\text{-}P)_f$	R_f ($\Omega\cdot cm^2$)	L (H)	R_L ($\Omega\cdot cm^2$)
25h	1.2E-5	0.84	5.6E3	2.0E4	1.2E4

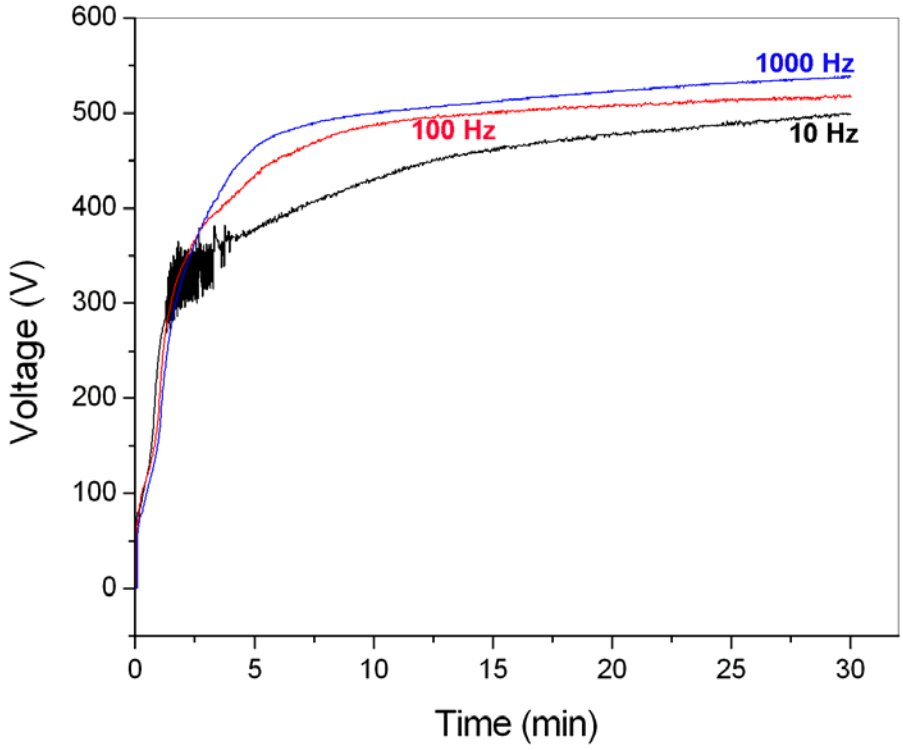

Figure 1 Voltage-time responses during PEO processing of AM50 magnesium alloy at three different frequencies

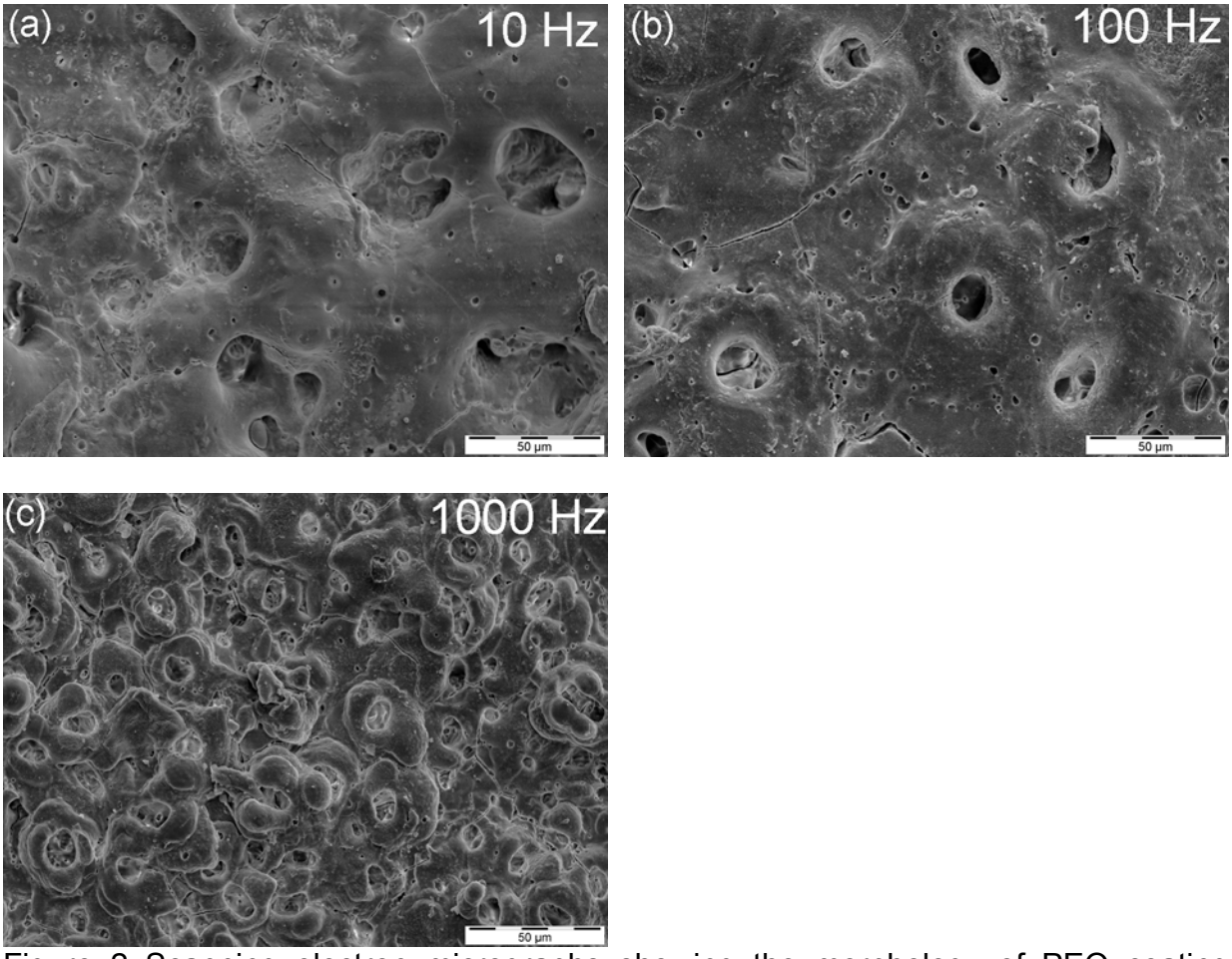

Figure 2 Scanning electron micrographs showing the morphology of PEO coatings obtained at three different frequencies

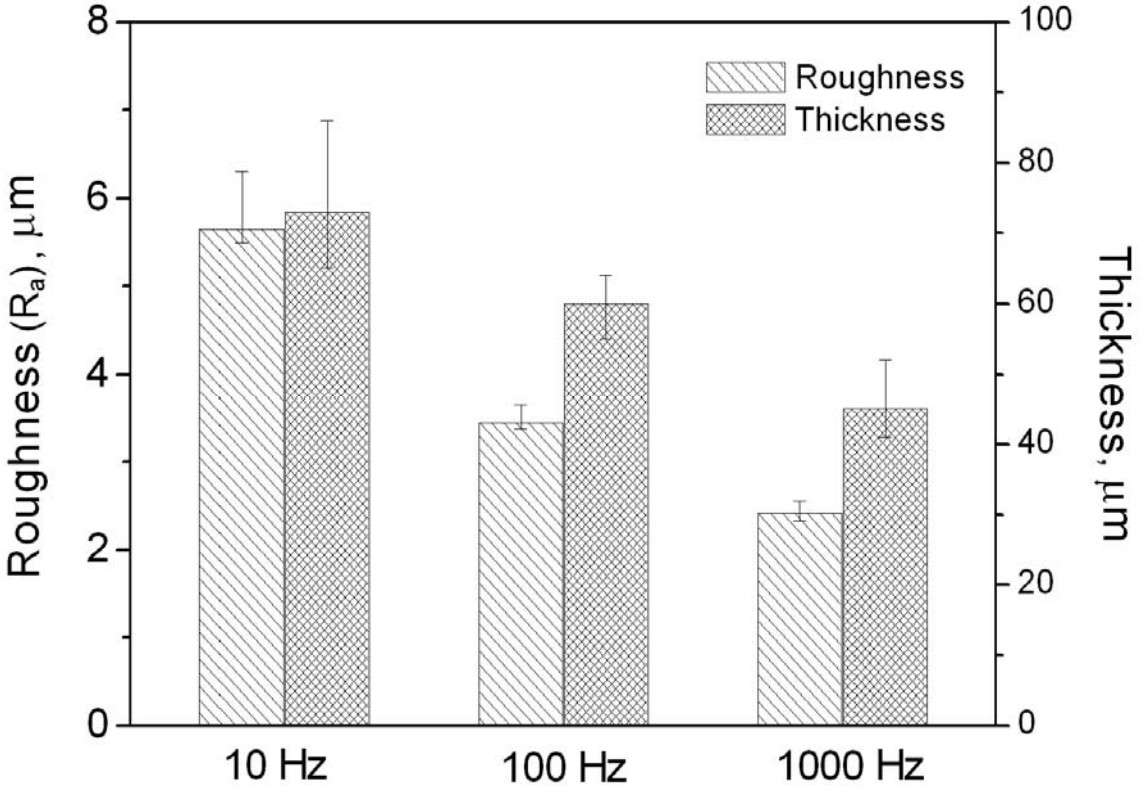

Figure 3 Effect of PEO processing frequency on the coating roughness and thickness

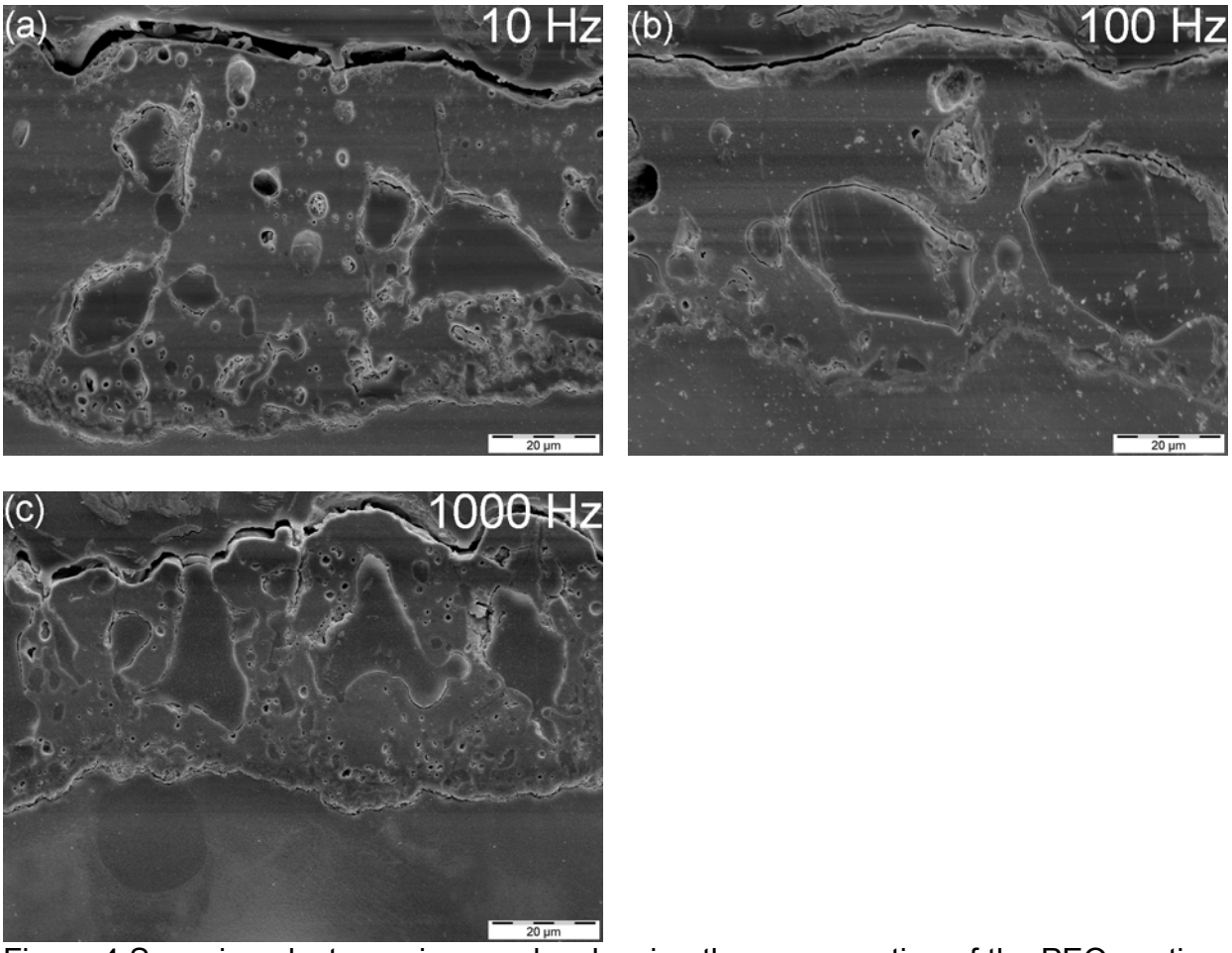

Figure 4 Scanning electron micrographs showing the cross-section of the PEO coatings obtained at three different frequencies

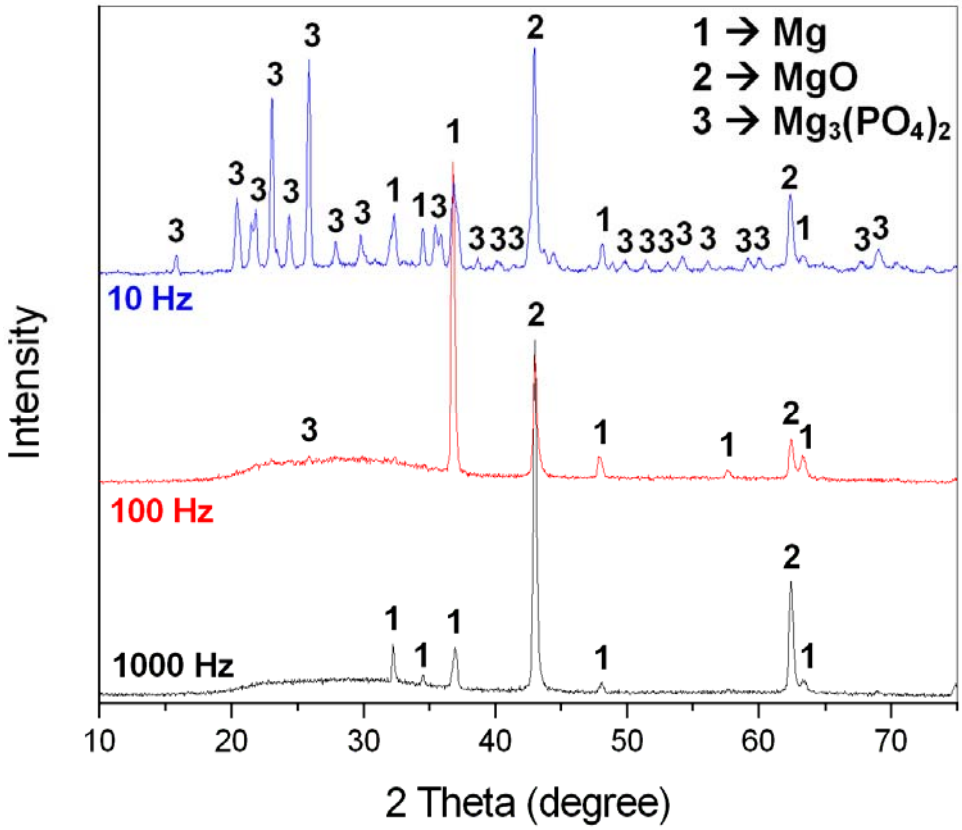

Figure 5 X-ray diffraction patterns for the PEO coated AM50 magnesium alloy at different frequencies

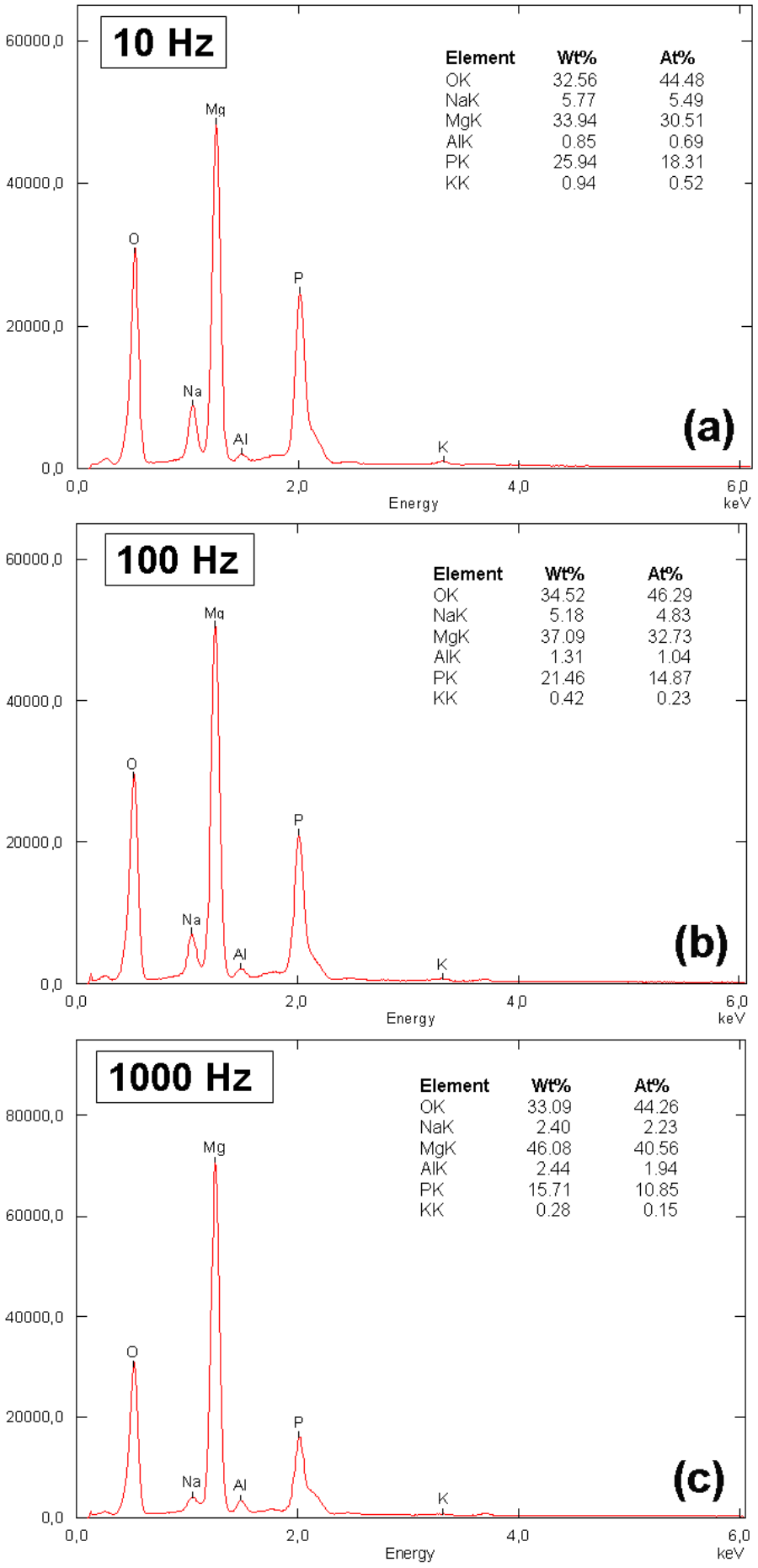

Figure 6 Energy dispersive spectra of the AM50 magnesium alloy specimens PEO coated at different frequencies

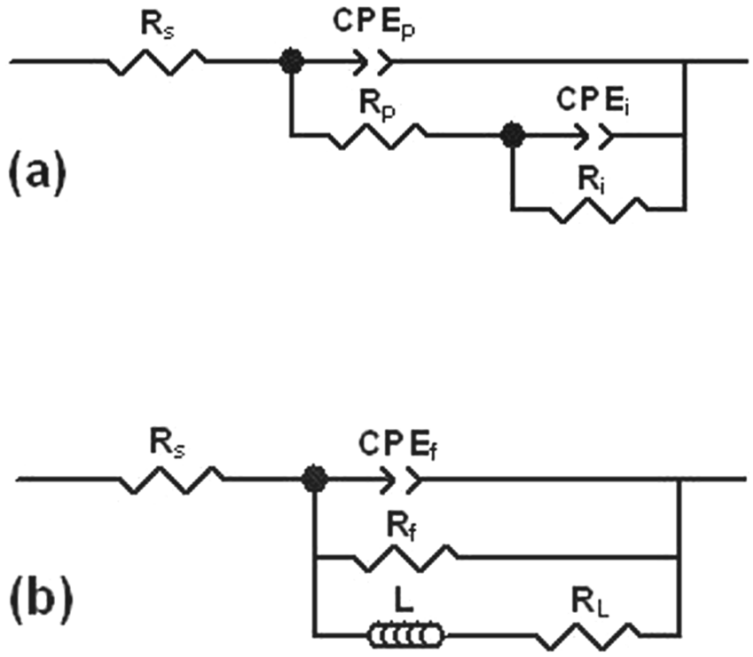

Figure 7 Equivalent circuit models for fitting the impedance data of PEO coating on AM50B magnesium alloy (a) immersion stage before localized corrosion failure and (b) immersion stage after localized corrosion failure.

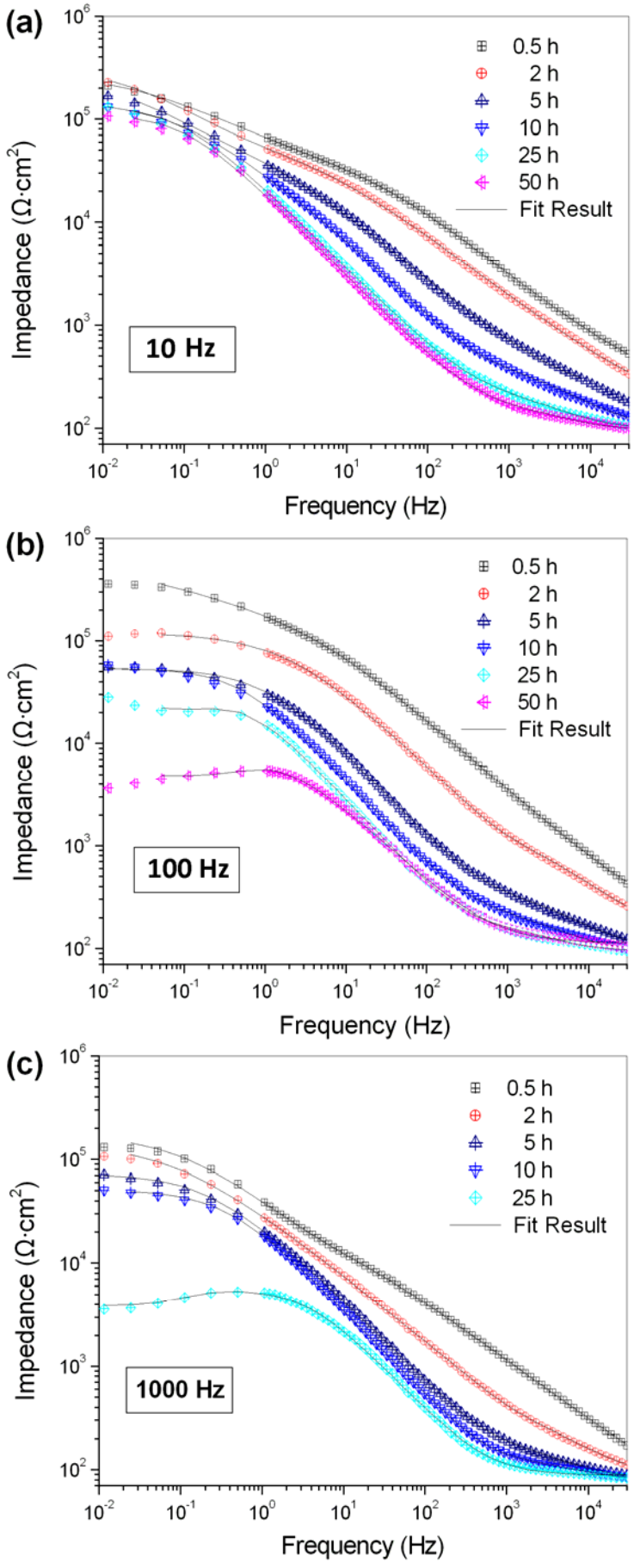

Figure 8 Bode plots obtained from EIS testing of the PEO coated AM50 alloy specimens (corrosive environment: 0.1 M NaCl)

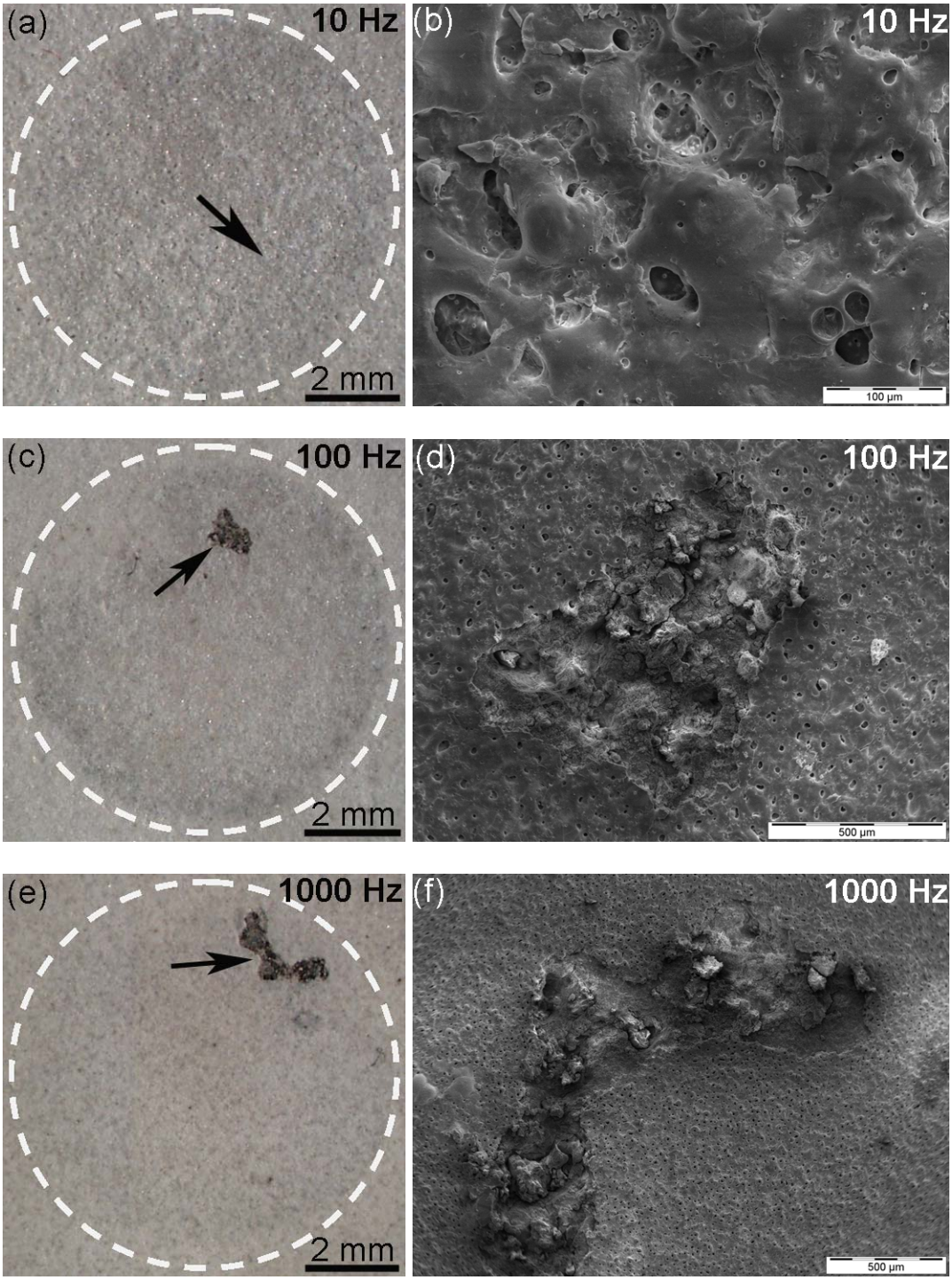

Figure 9 Optical macrographs of the EIS tested surface and the higher magnification scanning electron micrographs of the regions marked by arrows in the macrographs